

Bcl11a is required for neuronal morphogenesis and sensory circuit formation in dorsal spinal cord development

Anita John^{1,5,6,*}, Heike Brylka^{1,5,6}, Christoph Wiegrefe¹, Ruth Simon¹, Pentao Liu², René Jüttner⁶, E. Bryan Crenshaw, III³, Frank P. Luyten⁷, Nancy A. Jenkins^{4,‡}, Neal G. Copeland^{4,‡}, Carmen Birchmeier⁶ and Stefan Britsch^{1,5,6,§}

SUMMARY

Dorsal spinal cord neurons receive and integrate somatosensory information provided by neurons located in dorsal root ganglia. Here we demonstrate that dorsal spinal neurons require the Krüppel-C₂H₂ zinc-finger transcription factor Bcl11a for terminal differentiation and morphogenesis. The disrupted differentiation of dorsal spinal neurons observed in *Bcl11a* mutant mice interferes with their correct innervation by cutaneous sensory neurons. To understand the mechanism underlying the innervation deficit, we characterized changes in gene expression in the dorsal horn of *Bcl11a* mutants and identified dysregulated expression of the gene encoding secreted frizzled-related protein 3 (sFRP3, or *Frzb*). *Frzb* mutant mice show a deficit in the innervation of the spinal cord, suggesting that the dysregulated expression of *Frzb* can account in part for the phenotype of *Bcl11a* mutants. Thus, our genetic analysis of *Bcl11a* reveals essential functions of this transcription factor in neuronal morphogenesis and sensory wiring of the dorsal spinal cord and identifies *Frzb*, a component of the Wnt pathway, as a downstream acting molecule involved in this process.

KEY WORDS: Spinal cord, Transcription factor, Neuronal differentiation, Bcl11a (CTIP1), Mouse

INTRODUCTION

The ability of the nervous system to integrate and relay information relies on the coordinated development of neuronal circuits. An immense diversity of neuron types is created during development. Extrinsic and intrinsic mechanisms control their subsequent maturation and the establishment of functional connectivity. Connectivity relies on the presence of dendrites in postsynaptic neurons and on the cues that allow navigation of the axons of presynaptic neurons, both of which have to be precisely orchestrated to establish a functional neuronal circuitry (Marmigere and Ernfors, 2007; Dasen, 2009).

Somatosensory neurons and their target, the spinal cord, provide a model for the molecular analysis of neuronal circuit development (Vrieseling and Arber, 2006; Yoshida et al., 2006; Pecho-Vrieseling et al., 2009). During development of the dorsal spinal cord, different neuron types are generated from defined progenitor domains and subsequently become positioned in a highly organized laminar structure, the dorsal horn (Goulding et al., 2002; Helms and Johnson, 2003). Somatosensory neurons with cell bodies in dorsal root ganglia (DRG) innervate these spinal neurons, and

distinct sensory neuron types project to different spinal cord layers. For instance, nociceptive neurons project to the upper layers of the dorsal horn, whereas mechanosensory and proprioceptive neurons innervate deeper layers (Brown, 1981).

Transcriptional networks are essential for spatiotemporally correct neuronal differentiation and wiring in the spinal cord (reviewed by Dasen, 2009). For example, members of the Paired related, LIM homeobox or TLX families of transcription factors are involved in cell fate decisions, morphogenesis, positioning and wiring of dorsal spinal neurons (Chen et al., 2001; Qian et al., 2002; Cheng et al., 2004; Ding et al., 2004; Marmigere et al., 2006). The signals provided by dorsal horn neurons that guide sensory axons from DRG neurons to their spinal targets are incompletely defined. Several members of the Wnt pathway are expressed in the spinal cord. Wnts have been extensively demonstrated to possess axon guidance activity and to control neural circuit formation (reviewed by Salinas and Zou, 2008), making this pathway an attractive candidate regulator in the process of sensory wiring within the dorsal horn.

In a screen designed to identify novel candidate genes that control development of the somatosensory circuitry, we identified *Bcl11a* as a gene that is expressed in the dorsal horn of the spinal cord and in sensory neurons. *Bcl11a* (also known as *Evi9*, *Ctip1*) encodes a C₂H₂ zinc-finger transcription factor that acts as a transcriptional regulator through its interaction with COUP-TF proteins and through direct, sequence-dependent DNA binding (Avram et al., 2000). Bcl11a is expressed in lymphohematopoietic cells, in which it controls the development of B- and T-lymphocytes (Liu et al., 2003b) and the maintenance of mature erythroid cells (Sankaran et al., 2008; Sankaran et al., 2009). The close relative, Bcl11b, is required for differentiation of striatal neurons and the corticospinal tract (Arlotta et al., 2005; Arlotta et al., 2008). However, functions of Bcl11a in the somatosensory system have not been defined.

Here we show that Bcl11a is an important regulator of terminal neuronal differentiation and wiring. Mutation of *Bcl11a* in spinal neurons disrupts their maturation and morphogenesis,

¹Institute of Molecular and Cellular Anatomy, Ulm University, 89081 Ulm, Germany.

²The Wellcome Trust Sanger Institute, Hinxton, Cambridge CB10 1SA, UK.

³Mammalian Neurogenetics Group, Center for Childhood Communication, The Children's Hospital of Philadelphia, PA 19104, USA. ⁴Institute of Molecular and Cell Biology, 61 Biopolis Drive, Proteos, Singapore 138673. ⁵Georg-August-University, Center for Anatomy, 37075 Goettingen, Germany. ⁶Max Delbrück Center for Molecular Medicine (MDC), 13125 Berlin-Buch, Germany. ⁷Laboratory for Skeletal Development and Joint Disorders, Division of Rheumatology, Katholieke Universiteit Leuven, B-3000 Leuven, Belgium.

*Present address: Institute of Pharmacology and Toxicology, Biomedical Center, University of Bonn, 53105 Bonn, Germany

‡Present address: Cancer Research Program, The Methodist Hospital Research Institute, Houston, TX 77030, USA

§Author for correspondence (stefan.britsch@uni-ulm.de)

which is accompanied by defective innervation of the dorsal horn by somatosensory neurons. Among the genes dependent on *Bcl11a* for expression, we identified the Wnt antagonist secreted frizzled-related protein 3 (*sFRP3*, or *Frzb*) as a transcriptional target. Interestingly, we observe similar innervation deficits in the dorsal spinal cord of *Bcl11a* and *Frzb* mutants. Our findings show that *Bcl11a* is essential for sensory circuit formation and implicate *Frzb* in one aspect of the changes observed in *Bcl11a* mutant mice.

MATERIALS AND METHODS

Animals

To generate a conditional knockout allele (*Bcl11a^{lox}*) a neomycin resistance cassette was introduced at the 3' end of exon 1 of the *Bcl11a* gene. Exon 1 and the neomycin resistance cassette were flanked by loxP sites using previously described strategies (Liu et al., 2003a). Upon Cre-mediated recombination, exon 1 and the neomycin resistance cassette were excised from the *Bcl11a* locus, resulting in a null allele. To obtain mice with tissue-specific ablation of the *Bcl11a* allele, *Bcl11a^{lox/lox}* mice were crossed to either Deleter-Cre (Schwenk et al., 1995), *Brn4-Cre* (*Bcre-32* pedigree) (Wine-Lee et al., 2004) or Ht-PA-Cre (Pietri et al., 2003) transgenic mice. Homozygous mutants were compared with heterozygous littermates harboring a *Cre* allele. *Frzb* and *Sox10* mutant mice were described previously (Britsch et al., 2001; Lories et al., 2007). Mice were genotyped by PCR. All animal experiments were carried out in accordance with German law and were approved by the respective governmental offices in Berlin, Göttingen and Tübingen.

In situ hybridization, antibodies and histology

For in situ hybridization, spinal cords were dissected from mouse embryos at E14.5-18.5, fixed in 4% PFA and embedded in OCT compound (Sakura). Hybridizations were performed with DIG-labeled riboprobes on 18 μ m cryosections.

For immunofluorescence staining, tissue was fixed with 4% PFA in 0.1 M sodium phosphate buffer (pH 7.4). Cryosections (14 μ m) were obtained from matched cervical spinal cords. Stained sections were examined on a Zeiss LSM510 or Leica SP5II confocal microscope.

The following antibodies were used: rabbit and guinea pig anti-Lbx1 (Thomas Mueller, Berlin), rabbit anti-Ebfl1 (H. Wildner and C. Birchmeier, Berlin), guinea pig anti-Lmx1b (T. Jessel, New York), rabbit anti-TrkA (L. Reichardt, San Francisco), rabbit anti-CGRP (Chemicon), rabbit anti-parvalbumin (Chemicon), rabbit anti-aquaporin 1 (Chemicon), rabbit anti-MAP2 (Chemicon), mouse monoclonal anti-HuCD (Invitrogen), mouse monoclonal anti-tubulin (Sigma), and fluorophore-conjugated secondary antibodies (Dianova).

To generate an anti-*Bcl11a* antiserum, a 486 bp fragment of murine *Bcl11a* cDNA encoding amino acids 501-662 (NM_016707) was amplified by PCR and cloned into the bacterial expression vector pET-14b (Novagen), which provides the coding sequences for a His6 tag. His6-*Bcl11a* was propagated in BL21(DE3)pLysS cells, affinity purified on TALON metal resin (BD Biosciences) and injected into rabbits and guinea pigs (Charles River).

For anterograde labeling of sensory axons, segments of the vertebrate column with the spinal cord and DRG in loco were dissected from mutant and control embryos and fixed overnight in 4% PFA. DiI crystals (Invitrogen) were placed directly onto DRG, matched for their axial levels. DiI-loaded tissues were incubated at 37°C for up to 5 days. DiI tracings were examined on 80 μ m vibratome sections using a confocal microscope.

BrdU labeling of neurons and Golgi staining of spinal cord were carried out as described (Heimrich and Frotscher, 1991; Gross et al., 2002).

Cell counting

Cervical spinal cords matched for axial level from at least three mutant and control animals were sectioned serially (14 μ m). Cell numbers were counted on every fourth section. A total of three sections were evaluated per animal. Values are presented as mean \pm s.e.m. Differences were considered significant at $P < 0.05$ by Student's *t*-test.

Neuron cultures

Primary cultures from dorsal spinal cord neurons were established according to a modified previously published protocol (Banker and Goslin, 1998). Dorsal spinal horns were dissected from control and mutant embryos at E18.5. Cells were plated on poly-lysine-coated slides at $6-8 \times 10^4$ cells/ml. Neurons derived from the superficial dorsal horn were identified by expression of *Lmx1b* and cultured for up to 14 days in serum-free medium in the presence of 10 ng/ml NGF. For Sholl analysis (Sholl, 1953), images of individual neurons were overlaid with a grid of concentric circles, and the length and number of neurite branches were determined at 2.5 μ m intervals from the soma. Neuron cultures from three individual mutant and control animals and at least ten neurons per neuron culture were analyzed.

Electrophysiology

Whole-cell patch-clamp recordings of evoked excitatory postsynaptic currents (EPSCs) were performed as described (Liebel et al., 1997; Schmidt et al., 2007).

For slice preparation, cervical spinal cords from control and *Bcl11a* mutant animals were microdissected at E18.5 and embedded in agarose (2.5% SeaPlaque agarose, CAMBREX). Transverse slices (200 μ m) were prepared on a vibratome. During recordings, slices were perfused with a bath solution of 125 mM NaCl, 4 mM KCl, 10 mM glucose, 1.25 mM NaH_2PO_4 , 25 mM NaHCO_3 , 2 mM CaCl_2 , 1 mM MgCl_2 .

Numerical data are reported as mean \pm s.e.m. Statistical analysis was performed using StatView (SAS Institute). Student's *t*-test (two-tailed, unpaired; decay time, rise time, evoked EPSC) or χ^2 test (success rates, response rates) were used for statistical comparisons.

Microarray analysis

Microarray experiments were performed according to MIAME standards (Brazma et al., 2001) (<http://www.mged.org/Workgroups/MIAME/miame.html>). For each time point analyzed (E14.5 and E16.5), dorsal spinal cords from ten age-matched *Bcl11a* mutant (*Bcl11a^{lox/lox}; Brn4-Cre*) and ten control (*Bcl11a^{lox/+}; Brn4-Cre*) animals were used. Segments of the cervical spinal cord were dissected in ice-cold PBS and matched for axial level. To isolate their dorsal halves, we used the sulcus limitans as an anatomical landmark. After dissection, dorsal spinal cord segments were transferred to Trizol (Invitrogen). For RNA isolation, mutant and control tissue were pooled separately. cDNA synthesis and biotinylation of cRNA probes were carried out according to standard Affymetrix protocols with three technical replicates of mutant and control RNA, starting with 5 μ g total RNA for each replicate. From each replicate, 15 μ g of labeled cRNA were hybridized for 16 hours at 45°C to mouse Affymetrix MOE430 2.0 microarrays in a GeneChip hybridization oven 645. After hybridization, microarrays were washed and stained in a GeneChip fluidics station 450, and scanned on a GeneChip scanner 3000 7G. Raw data analysis was performed using Bioconductor software (www.bioconductor.org). Quality of hybridization results was assessed with the affyPLM Bioconductor tool. After GC-RMA normalization of data, \log_2 signal intensity was used for value definition.

Quantitative real-time RT-PCR

Total RNA was prepared from dorsal spinal cord of controls and *Bcl11a* mutants using the RNeasy Mini kit (Qiagen). RNAs were reverse transcribed with Superscript II reverse transcriptase (Invitrogen) and quantitative real-time PCR (qRT-PCR) was performed using the QuantiTect SYBR Green PCR kit (Qiagen) in a LightCycler 480 system (Roche). The following oligonucleotides (5'-3') were used: *Frzb*, GCTGAGAA-GTGGGAAGGATCG and AACTGTGCGGTTTTCTTTG; *Gapdh*, CCAGAGCTGAACGGGAAG and TGCTGTTGAAGTCGCAGG. The relative copy number of *Gapdh* RNA was quantified and used for normalization. Data were analyzed using the $2^{-\Delta\Delta C_t}$ method (Livak and Schmittgen, 2001).

Chromatin immunoprecipitation (ChIP) on embryos

ChIP assays were performed on wild-type dorsal spinal cords collected from ten embryos at E14.5 using the EpiQuik Tissue Chromatin Immunoprecipitation kit (Epigentek, Framingham, MA, USA) including

specific antibodies recognizing RNA polymerase II and mouse IgG as controls. Every ChIP was replicated at least three times. The precipitated DNA was analyzed by quantitative PCR using oligonucleotides (5'-3') that recognize the promoter regions of: *Gapdh*, AAGGCTGGTGTGTGGAGAACTG and GTCCCCTTGCAACATACATAACTG; *Frzb* promoter region 1 (Frzb1), GAGCAGCCAGGACTAGCAAC and ACCTGGGAGCACTTGGATC; *Frzb* promoter region 2 (Frzb2), TTGAGTTTTTCAGGGGACTGG and TCTCTGTGGTGCCTTGAGAG; *Frzb* promoter region 3 (Frzb3), ACCATTGAGCAGAGGGATTG and TTCCCTAAGTGCCATTGAGC; *Drg11*, TCAAATGCCCTACTGCTCCT and GGGACTGCCAGAAATTGATA. All primer sets were tested by PCR using input and genomic DNA (supplementary material Fig. S4). Promoter regions for *Frzb* and *Drg11* were selected using ensembl.org, avoiding known RNA polymerase II binding sites. The promoter fragment for *Gapdh* specifically flanks the TATA box of this gene (Iankova et al., 2006). ChIP-qPCR results were analyzed by determining the amount of precipitated DNA as a percentage of input DNA. Data of three independent ChIP assays were pooled, mean±s.e.m. was calculated and statistical analysis performed using Student's *t*-test.

RESULTS

Expression and conditional mutation of *Bcl11a* in the spinal cord

In mice, at least three different isoforms, termed Evi9a, b and c, are generated from the *Bcl11a* gene (Nakamura et al., 2000). To analyze expression of *Bcl11a*, we generated antibodies against a 161 amino acid fragment of *Bcl11a* that is present in the Evi9a and b isoforms, but not in Evi9c (Fig. 1D-F; supplementary material Fig. S1), and performed in situ hybridizations with pan-specific (Fig. 1A-C) and isoform-specific (Fig. 1G-I) riboprobes. *Bcl11a* transcript and protein were first detected at E11.0 and E11.5, respectively, in the mantle zone of the most superficial dorsal neural tube, and, albeit at much lower levels, within a few cells of the ventricular zone (Fig. 1A,D). With ongoing development, *Bcl11a* was expressed by the majority of postmitotic dorsal spinal neurons, and at E18 81.47±2.41% of cells expressing the pan-neuronal marker HuC/D co-express *Bcl11a* within the dorsal horn (Fig. 1B,C,E,F,K; supplementary material Fig. S1). All three isoforms of *Bcl11a* were detected in the spinal cord. Unlike *Evi9b*, *Evi9a* and *Evi9c* expression appeared in almost identical patterns restricted to the dorsal spinal cord (Fig. 1G-I). In addition, *Bcl11a* was expressed by the majority of primary sensory neurons in DRG, as well as in a few cells in the ventral neural tube, some of which co-express *Isl1* and appear to represent differentiating motoneurons (Fig. 1D,E; data not shown).

Mice with a null mutation in *Bcl11a* show defects in lymphopoiesis and die shortly after birth (Liu et al., 2003b). To define functions of *Bcl11a* in neurons and to distinguish functions in presynaptic primary sensory neurons from those in postsynaptic dorsal spinal neurons we employed the Cre/loxP system (Fig. 1L-N). Homozygous mutant offspring from floxed *Bcl11a* mice crossed to a Deleter-Cre (*Del-Cre*) mouse strain (Schwenk et al., 1995) died within a few hours after birth and were indistinguishable from *Bcl11a* null mutants (Liu et al., 2003b). *Bcl11a* protein expression was undetectable in such mice (Fig. 1N). In situ hybridization with isoform-specific probes demonstrated the absence of *Evi9c* transcripts in the *Bcl11a* mutants (Fig. 1J). When floxed *Bcl11a* mice were crossed to *Brn4-Cre* mice that express *Cre* in neurons of the central but not of the peripheral nervous system (Wine-Lee et al., 2004), *Bcl11a* expression was eliminated from spinal neurons but not in primary sensory neurons within DRG (Fig. 1L). Crossing floxed *Bcl11a* mice to an *Ht-PA-Cre* mouse line, in which *Cre* is active in neural crest cells and their derivatives (Pietri et al., 2003; Yoshida et

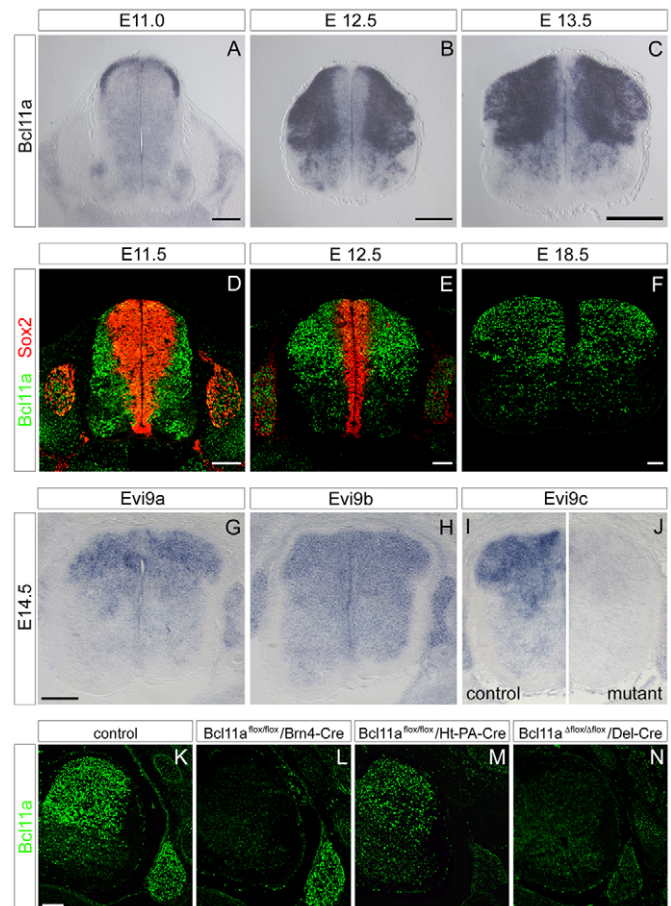


Fig. 1. Expression analysis and conditional mutation of *Bcl11a* in the spinal cord. (A-F) In situ hybridization (A-C) and immunohistological analysis (D-F) of *Bcl11a* expression in the embryonic spinal cord at different developmental stages using *Bcl11a*-specific probes and antibodies, respectively. The ventricular zone was visualized with antibodies against Sox2 (D,E). (G-J) In situ hybridizations using *Evi9a* (G), *Evi9b* (H) and *Evi9c* (I,J) specific probes on wild-type (G-I) or *Bcl11a* mutant (J) spinal cord sections of E14.5 embryos. (K-N) Immunohistological analysis of spinal cord and dorsal root ganglia (DRG) on transverse sections of control (K), *Bcl11a*^{flox/flox};*Brn4-Cre* (L), *Bcl11a*^{flox/flox};*Ht-PA-Cre* (M) and *Bcl11a*^{flox/flox};*Del-Cre* (N) mouse embryos at E15.5 using antibodies against *Bcl11a*. Scale bars: 100 µm.

al., 2006), completely abolished *Bcl11a* expression in primary sensory neurons, whereas *Bcl11a* expression was preserved in most of the dorsal spinal neurons (Fig. 1M).

***Bcl11a* is required for terminal differentiation and morphogenesis of dorsal spinal neurons**

Analysis of dorsal spinal neurons of *Brn4-Cre*;*Bcl11a* mice revealed changes in differentiation that were first apparent at E14.5. In control mice, neurons of the superficial dorsal horn express the transcription factors *Lmx1b*, *Ebf1*, *Drg11* (Prrxl1 – Mouse Genome Informatics) and *Pax2*, with a few *Lbx1*-positive cells intermingled (Fig. 2A,C,E; supplementary material Fig. S2). This region corresponds to layers I and II in the adult spinal cord and is innervated by cutaneous sensory afferents from DRG. During this period, *Bcl11a* is expressed by the majority of postmitotic neurons of the dorsal spinal horn, with *Evi9a* and *Evi9c* being more restricted to the superficial zone, and overlaps with *Lmx1b*

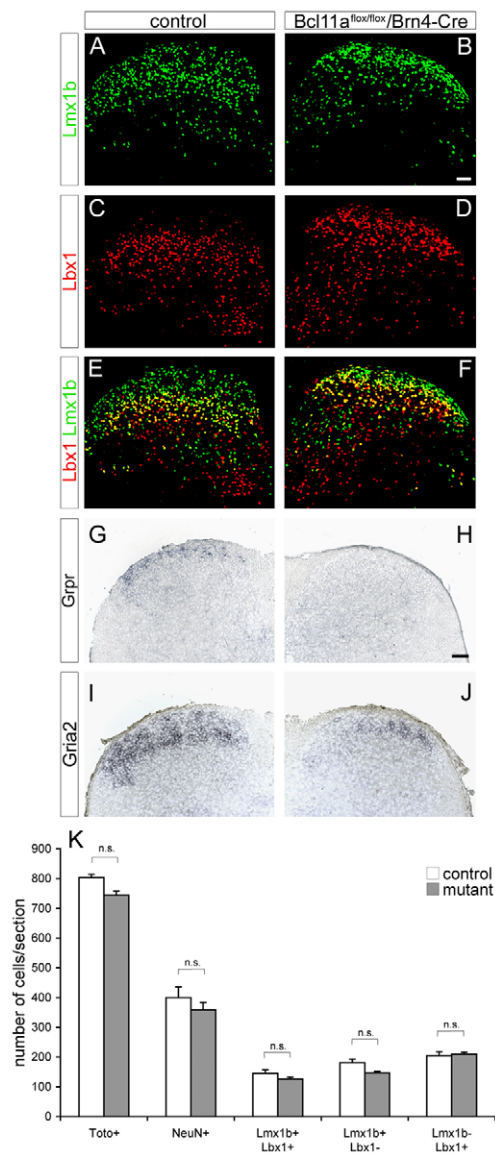


Fig. 2. Analysis of neuronal differentiation in the *Bcl11a* mutant dorsal spinal cord. (A-F) Immunohistological analysis on dorsal spinal cord sections from control (A,C,E) and *Bcl11a*^{flx/flx};*Brn4-Cre* (B,D,F) mice at E18.5 using antibodies against Lmx1b (A,B,E,F) or Lbx1 (C-F). (G-J) In situ hybridization analysis on dorsal spinal cord sections from control (G,I) and *Bcl11a* mutant (H,J) animals at E18.5, with probes specific for *Grpr* (G,H) and *Gria2* (I,J). (K) Numbers of cells (Toto⁺), neurons (NeuN⁺) and of marker-defined neuron populations in the dorsal horn of *Bcl11a* mutant and control embryos. Mean ± s.e.m. n.s., not significant. Scale bars: 50 μm.

expression (Fig. 1C,F,G,I; supplementary material Fig. S1). In *Brn4-Cre*;*Bcl11a* mutants the superficial zone was invariably compressed, with the positions of the deeper layers shifted superficially. Lmx1b⁺, Ebf1⁺ or Drg11⁺ nuclei within this zone appeared compacted when compared with controls (Fig. 2B,D,F; supplementary material Fig. S2A-D). To explore whether this phenotype is caused by changes in the size of specific neuron populations we determined the numbers of Toto⁺, NeuN⁺, Lbx1⁺ or Lmx1b⁺ cells within the dorsal horn. Total neuron numbers, as well as those of individual neuron populations, were unchanged in mutants (Fig. 2K). Pulse labeling with BrdU during late phase

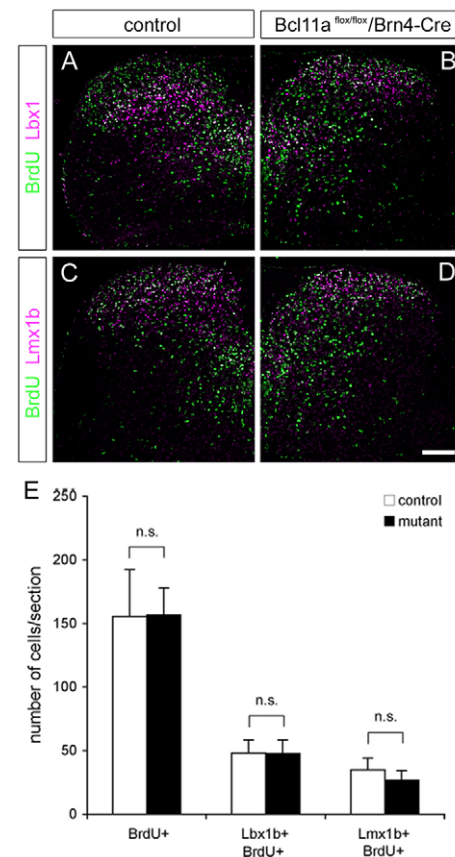


Fig. 3. Birthdating and tracing of *Bcl11a* mutant dorsal spinal neurons. (A-D) Immunohistochemical analysis of dorsal spinal cord on transverse sections of control (A,C) and *Bcl11a*^{flx/flx};*Brn4-Cre* (B,D) mice that received a single dose of BrdU at E11.5 and were sacrificed at E16.5 using antibodies against BrdU (A-D), Lbx1 (A,B) and Lmx1b (C,D). (E) Numbers of BrdU⁺, Lbx1⁺ BrdU⁺ and Lmx1b⁺ BrdU⁺ cells in the spinal cord of *Bcl11a* mutant and control embryos. Mean ± s.e.m. n.s., not significant. Scale bar: 100 μm.

neurogenesis (Gross et al., 2002; Muller et al., 2002) revealed normal birth rates and migratory capacities of *Bcl11a* mutant dorsal spinal neurons (Fig. 3A-E). With ongoing development, neurons of the superficial dorsal horn express late differentiation markers, such as gastrin releasing peptide receptor (*Grpr*), galanin and *Gria2* (Baccei and Fitzgerald, 2004; Sun and Chen, 2007; Xu et al., 2008). Expression of these genes was greatly reduced (*Gria2*) or undetectable (*Grpr*, galanin) in mutants (Fig. 2G-J; data not shown), suggesting that neurons within the superficial dorsal horn require *Bcl11a* for terminal differentiation.

The compaction of neurons within the superficial dorsal horn might be caused by a reduced neuropil. To test this, we defined the expression of the microtubule-associated protein MAP2 (Mtap2 – Mouse Genome Informatics) (Ding et al., 2004). Compared with controls, MAP2 expression was greatly reduced in the superficial dorsal horn of *Bcl11a* mutant mice (Fig. 4A,B). At E18.5, Golgi-stained neurons in the dorsal horn of controls frequently display complex neurite trees (Fig. 4C). In homozygous mutants, neurites were severely reduced, and remaining structures often appeared misshapen (Fig. 4D). To quantify neurite formation in spinal neurons, we cultured primary neurons from superficial dorsal horn tissues and carried out a Sholl analysis (Fig. 4E-G). Viability and plating efficiency of mutant and control spinal neurons were

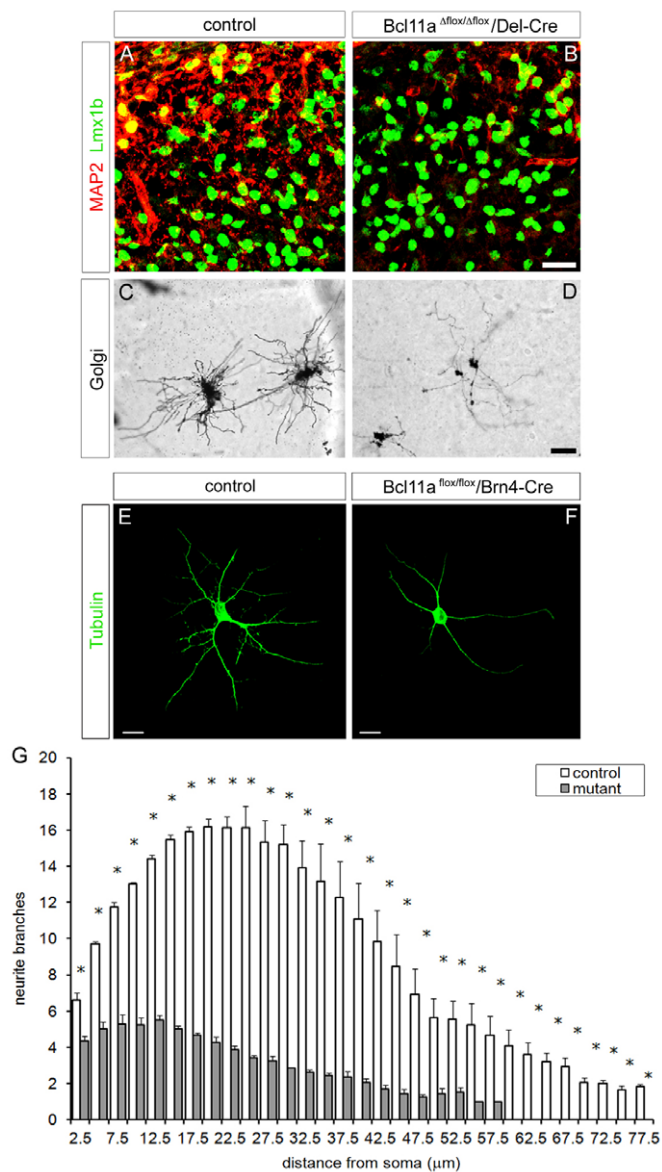


Fig. 4. Dorsal spinal neurons require Bcl11a for morphogenesis. (A-D) Transverse sections of the superficial dorsal horn of control (A,C) and Del-Cre recombined *Bcl11a* mutant (B,D) mice. Note that in mutants, Lmx1b-expressing neurons are more densely packed (B). Neurite morphology of control (C) and *Bcl11a* mutant (D) neurons in the superficial dorsal horn at E18.5 was visualized by Golgi staining. (E,F) Primary neuron cultures derived from dorsal spinal cord tissues of E18.5 control (E) and *Bcl11a* mutant (F) animals stained with anti-tubulin antibodies. (G) Sholl analysis of neurite length and arborization. Mean \pm s.e.m. *, $P < 0.05$ (Student's *t*-test). Scale bars: 20 μ m in B; 30 μ m in D; 40 μ m in E,F.

comparable. However, the overall number, length and branching frequency of neurites were significantly reduced in *Bcl11a* mutant neurons (Fig. 4G).

Primary sensory neurons require postsynaptic Bcl11a expression for correct wiring

Bcl11a is expressed in both presynaptic sensory neurons and postsynaptic spinal target neurons (Fig. 1). We next asked whether Bcl11a is required for correct wiring, and if so, on which site.

Central axons of sensory neurons were labeled at E16.5 with DiI. In the superficial dorsal horns of *Brn4-Cre;Bcl11a* mutants, the density of DiI-positive fibers was greatly reduced and the remaining fibers appeared disorganized. Only a few axons crossing the midline or located in a dorsolateral region of the dorsal horn were detectable by DiI labeling in mutants (Fig. 5A,B). TrkA (Ntrk1 – Mouse Genome Informatics) -positive nociceptive fibers preferentially terminate in the superficial dorsal horn. Immunohistological analysis with antibodies against TrkA or aquaporin 1, a water channel protein that is expressed by small-diameter nociceptive fibers (Oshio et al., 2006), invariably revealed almost complete loss of such fibers in the dorsal horn of *Brn4-Cre;Bcl11a* mutants (Fig. 5C-F). Similar results were obtained with antibodies against CGRP (Calca – Mouse Genome Informatics), which marks a specific subset of peptidergic neurons terminating in the superficial dorsal horn (Fig. 5G,H). By contrast, parvalbumin-positive proprioceptive neurons projecting to the ventral spinal cord, where most neurons do not express Bcl11a (Fig. 1F,G,I), were unaffected by the mutation (Fig. 5I,J). Similar phenotypes were observed in spinal cords at E13.5 and E14.5, when cutaneous sensory afferents begin to grow into the dorsal horn (not shown). To exclude the possibility that the observed phenotype resulted from degeneration or aberrant differentiation of primary sensory neurons, we determined the numbers and apoptosis rates of TrkA-positive and parvalbumin-positive neurons within DRG. We did not observe any differences in apoptosis or in the size of individual neuron populations between *Brn4-Cre;Bcl11a* mutants and controls (Fig. 5K-P; data not shown).

To assess directly whether synaptic input from cutaneous sensory afferents to mutant dorsal spinal neurons was reduced, we recorded postsynaptic currents in dorsal horn neurons elicited by extracellular stimulation at the dorsal root entry zone (Fig. 5Q). Basic synaptic properties, such as amplitude, decay time constant (control: 3.86 ± 0.70 mseconds, $n=12$; mutant: 3.55 ± 0.41 mseconds, $n=14$) and rise time (control: 1.72 ± 0.24 mseconds, $n=12$; mutant: 1.74 ± 0.21 mseconds, $n=14$) were similar in mutant and control neurons (supplementary material Fig. S3A,B). In addition, paired-pulse properties, a commonly used criterion for presynaptic alterations, were unchanged in mutants (supplementary material Fig. S3C,D). However, the success rates of evoked excitatory postsynaptic currents (EPSCs) in dorsal horn neurons were significantly reduced ($P < 0.05$) from 76.0% in controls to 52.4% in mutants (Fig. 5R).

When we analyzed *Ht-PA-Cre;Bcl11a* mutants at E18.5, TrkA-positive and aquaporin 1-positive axon projections were unchanged (Fig. 6C,D; data not shown). In addition, the primordial layer architecture in *Ht-PA-Cre;Bcl11a* mutants was indistinguishable from that of controls (Fig. 6A,B). Together, this indicates that Bcl11a is required in spinal target neurons, but is dispensable in presynaptic sensory neurons, for correct wiring and differentiation in the superficial dorsal horn.

The phenotype observed in *Bcl11a* mutant spinal cords does not exclude the possibility that impaired differentiation and morphogenesis of dorsal spinal neurons are caused indirectly by deficits in sensory innervation. To test this we analyzed *Sox10* mutant mice. In such mice, primary sensory neurons are eliminated before E12.5 by apoptosis (Britsch et al., 2001), allowing an assessment of dorsal horn development in the absence of sensory input (Fig. 6G,H). In *Sox10* mutants, expression of Lbx1, Lmx1b, Gria2 and Grpr, primordial layer architecture and neuron morphology as determined by Golgi and MAP2 staining were unchanged (Fig. 6E,F,I-N; data not shown). Thus, the defective

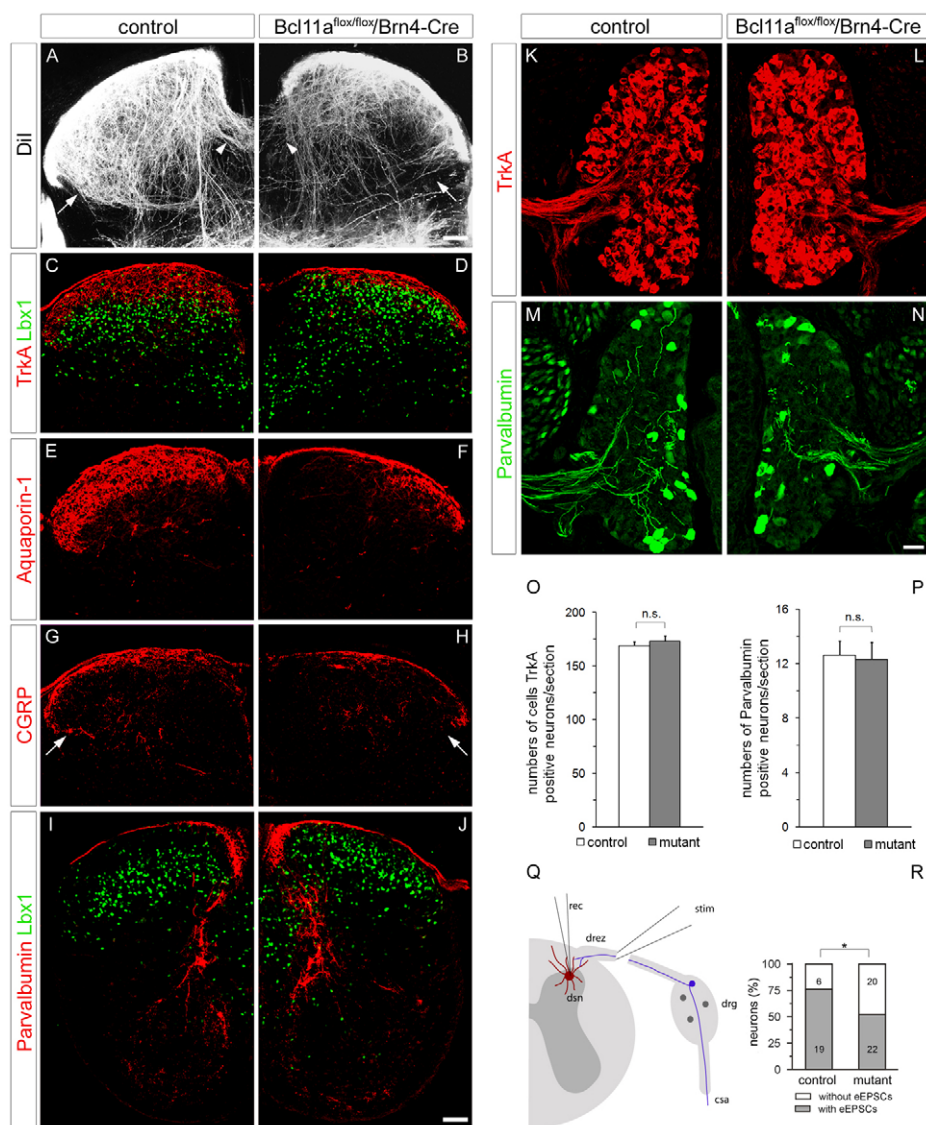


Fig. 5. Sensory axon projections in the *Bcl11a* mutant dorsal spinal horn.

(A–J) Transverse sections of the dorsal horn of control (A, C, E, G, I) and Brn4-Cre recombinant *Bcl11a* mutant (B, D, F, H, J) mice at E16.5 (A, B) and E18.5 (C–J). Sensory axons were traced with Dil (A, B). Axons crossing the midline are marked (arrowheads in A, B). Residual fibers are disorganized (arrows in A, B). A similar phenotype is detectable with anti-CGRP staining (arrows in G, H). (C–J) Immunohistological analysis of sensory axons projecting into the spinal cord with antibodies against TrkA (C, D), aquaporin 1 (E, F), CGRP (G, H) and parvalbumin (I, J). (K–P) Immunohistological detection (K–N) and quantification (O, P) of TrkA-positive (K, L, O) and parvalbumin-positive (M, N, P) sensory neurons in DRG. Mean ± s.e.m. n.s., not significant. (Q, R) Electrophysiological analysis of evoked excitatory postsynaptic currents (eEPSCs) from dorsal horn neurons of control and Brn4-Cre recombinant *Bcl11a* mutants at E18.5. *, $P < 0.05$ (Fisher's exact test). rec, recording pipette; stim, stimulation pipette; dsn, dorsal spinal neuron; drez, dorsal root entry zone; drg, dorsal root ganglion; csa, central sensory axon. Scale bars: 50 μ m.

neuronal differentiation and morphogenesis as observed in the *Bcl11a* mutant dorsal horn is independent of defective sensory innervation.

Dysregulated expression of *Frzb* accounts in part for the disrupted innervation of the *Bcl11a* mutant spinal cord

To identify genes that are differentially expressed in *Bcl11a* mutants, we performed microarray analyses on dorsal spinal cord tissues of E14.5 and E16.5 embryos. Analysis of E16.5 embryos revealed that the expression of 20 and 121 genes was significantly downregulated and upregulated, respectively (change $P \leq 0.0001$; fold change ≤ -1.9 and ≥ 1.9 ; supplementary material Table S1). In accordance with a function in terminal differentiation (see above), *Gria2* and *Grpr* were significantly downregulated in mutants at E16.5 but not E14.5 (Table 1; see Fig. 2).

The gene encoding the extracellular signaling molecule secreted frizzled-related protein 3 (*Frzb*) was most consistently downregulated according to our microarray analyses (Table 1; supplementary material Table S1). As members of the sFRP family can act as guidance cues for navigating axons (Rodriguez et al.,

2005), we focused on this candidate for further analysis. In situ hybridization verified downregulation of *Frzb* in the *Bcl11a* mutant spinal cord (Fig. 7A, B), and *Frzb* mRNA was 5.6-fold downregulated in qRT-PCR of *Bcl11a* mutant dorsal horn tissue ($P < 0.01$; Fig. 7C). *Frzb* expression was unchanged in *Sox10* mutant dorsal horn, excluding downregulation of *Frzb* secondary to defective sensory innervation (Fig. 6O, P).

To test whether *Frzb* is directly regulated by Bcl11a, we performed ChIP on embryos; the specificity of the Bcl11a antibody was verified by western blot analysis (Jawaid et al., 2010). The Bcl11a antibody specifically precipitated two promoter fragments, corresponding to +623 to +849 (Frzb1) and -27 and +138 (Frzb2) relative to the transcription initiation site of *Frzb* (Fig. 7D, E). The amount of recovered Frzb1 and Frzb2 promoter DNA was significantly higher than with control IgG (Frzb1, Bcl11a antibody 0.233 ± 0.02% and IgG 0.14 ± 0.032% of input DNA; Frzb2, Bcl11a antibody 0.307 ± 0.047% and IgG 0.12 ± 0.03% of input DNA; $P < 0.05$; Fig. 7D, E). No specific binding of Bcl11a to a distant fragment comprising -786 to -1008 was detected (Frzb3, Bcl11a antibody 0.009 ± 0.0005% and IgG 0.03 ± 0.02% of input DNA; Fig. 7D, E).

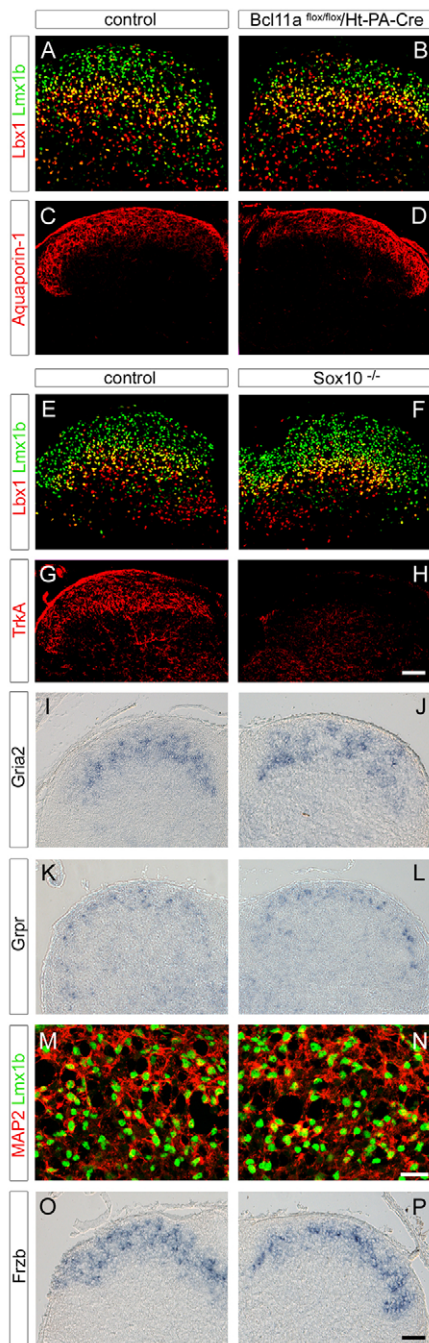


Fig. 6. Analysis of dorsal spinal cords of Ht-PA-Cre recombinated *Bcl11a* mutants and of *Sox10* mutants. (A-P) Transverse sections of the dorsal horn from control (A,C,E,G,I,K,M,O), Ht-PA-Cre recombinated *Bcl11a* mutant (B,D) and *Sox10* mutant (F,H,J,L,N,P) mice at E18.5, stained with antibodies against Lmx1b (A,B,E,F,M,N), Lbx1 (A,B,E,F), aquaporin 1 (C,D), TrkA (G,H) and MAP2 (M,N), or hybridized with probes against *Gria2* (I,J), *Grpr* (K,L) and *Frzb* (O,P). (M,N) High magnifications of the superficial zones of dorsal horns from controls (M) and *Sox10* mutants (N). Scale bars: 50 μ m in H,P; 20 μ m in N.

To validate the ChIP assays, an antibody against RNA polymerase II and a PCR strategy amplifying a *Gapdh* promoter fragment that flanks the TATA box were used (Iankova et al., 2006). We recovered significantly more *Gapdh* promoter DNA using the antibody directed against RNA polymerase II than with

the IgG control; no significant enrichment of *Gapdh* promoter DNA was obtained with *Bcl11a* antibodies (*Gapdh*, RNA polymerase II antibody 0.51 \pm 0.038% and IgG 0.1 \pm 0.05% of input DNA, $P < 0.05$; *Bcl11a* antibody 0.04 \pm 0.02% of input DNA; Fig. 7D,E). In addition, we used primers amplifying a promoter sequence of *Drg11*, which is expressed in dorsal horn neurons but is unaffected by the *Bcl11a* mutation (supplementary material Fig. S2). No significant recovery of *Drg11* promoter DNA was observed with *Bcl11a* antibodies when compared with the IgG control (Fig. 7E). Neither the *Frzb*1-3 nor the *Drg11* fragments used for ChIP contain a TATA box or other known RNA polymerase II binding sites. Accordingly, no significant precipitation of these fragments was observed with RNA polymerase II antibodies (Fig. 7E).

Analyzing the DNA sequence of the precipitated *Frzb* promoter region 1 revealed putative *Bcl11a* binding sites GGCCGG (starting at +824) and GGCCGC (starting at +796), both of which display high similarity to the previously described consensus binding motif of *Bcl11a* (Avram et al., 2002; Chen et al., 2009). Furthermore, a transgenic *Frzb* promoter fragment (indicated in Fig. 7D) lacking region 1 has been shown to recapitulate endogenous *Frzb* expression in mice, except in neural tube (Tylzanowski et al., 2004), supporting the assertion that interaction of *Bcl11a* protein with *Frzb* promoter region 1 is functional in neurons.

To assess whether *Frzb* is required for sensory innervation of the dorsal horn, we analyzed *Frzb* mutant mice (Lories et al., 2007) (Fig. 8A,B). In the dorsal horn of *Frzb* mutants we observed a reduction in TrkA and aquaporin 1 but not in parvalbumin expression (Fig. 8E-J). The reduction in the innervation of TrkA⁺ and aquaporin 1⁺ sensory neurons was less pronounced than observed in *Bcl11a* mutants. DiI labeling of primary sensory axons revealed reduced and disorganized sensory innervation of the dorsal horn of *Frzb* mutants (Fig. 8C,D). *Frzb* is also expressed in some sensory neurons (Fig. 8K,L). In mutants, the numbers and distribution of TrkA⁺ and parvalbumin⁺ neurons within DRG were normal (Fig. 8M-R). The primordial layer architecture, differentiation and morphology of dorsal spinal neurons were unchanged in *Frzb* mutants as assessed by expression of Lbx1, Lmx1b, Grpr and *Gria2* and by Golgi and MAP2 staining (supplementary material Fig. S5A-J). We conclude that the dysregulated *Frzb* expression can in part account for the disrupted sensory innervation of the *Bcl11a* mutant spinal cord.

DISCUSSION

The dorsal spinal cord processes somatosensory information and relays it to higher brain centers. In this study, we provide genetic evidence that the zinc-finger transcription factor *Bcl11a* is essential for the correct sensory innervation of the dorsal spinal cord. This function of *Bcl11a* is in part mediated by its role in the transcriptional control of *Frzb*.

***Bcl11a* is required for sensory circuit formation**

Small-diameter cutaneous sensory afferents are greatly reduced in the dorsal horn of *Bcl11a* mutant mice. Similar phenotypes have been reported for mice with a mutation of the transcription factors *Lmx1b*, *Drg11* or *Tlx3/Tlx1* (Chen et al., 2001; Qian et al., 2002; Ding et al., 2004). These genes are expressed by the same neuron type and overlap in part with the expression of *Bcl11a* in the dorsal horn (supplementary material Fig. S1), raising the question of whether *Bcl11a* exerts part of its functions through a shared genetic program. However, the expression patterns of *Lmx1b* and *Drg11*

Table 1. Summary of microarray gene expression analysis in the dorsal spinal cord of control (*Bcl11a*^{flox/+};*Brn4-Cre*) and *Bcl11a* mutant (*Bcl11a*^{flox/flox};*Brn4-Cre*) mice at E14.5 and E16.5

| Gene symbol | Gene name | Fold change | |
|------------------------------|---|-------------|----------|
| | | E14.5 | E16.5 |
| <i>Bcl11a</i> | B cell CLL/lymphoma 11A | -7.5*** | -13.5*** |
| Neurotransmission | | | |
| <i>Grpr</i> | gastrin releasing peptide receptor | nd | -6.2*** |
| <i>Gria2</i> | glutamate receptor, ionotropic, AMPA2 (alpha 2) | nd | -1.9*** |
| Signaling | | | |
| <i>Frzb</i> (<i>sFRP3</i>) | secreted frizzled-related protein 3 | -3.0*** | -2.2*** |

Average signal fold changes and change *P*-values (***, *P*≤0.0001) from three independent replicates are shown. Genes downregulated in *Bcl11a* mutant dorsal spinal cord are indicated by negative values. Only those genes verified by in situ hybridization, qRT-PCR and/or ChIP are shown. nd, expression not detected.

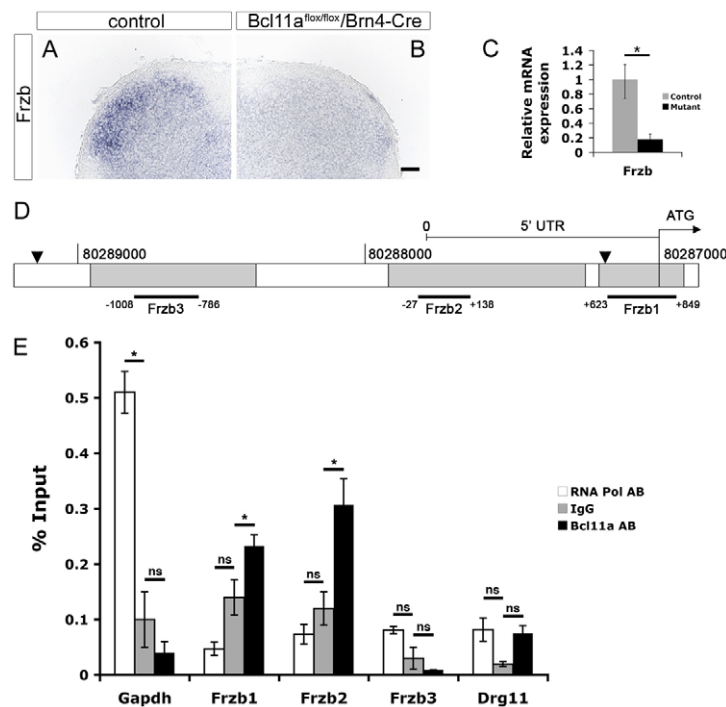
as well as the number of *Lmx1b*-positive dorsal neurons were unchanged in *Bcl11a* mutants. Whereas we observed defects in the terminal differentiation of dorsal neurons in *Bcl11a* mutants, changes in neuron type composition and neuronal fate have been detected in the dorsal horns of *Lmx1b* and *Tlx3/Tlx1* mutant animals (Qian et al., 2002; Cheng et al., 2004; Ding et al., 2004).

Bcl11a is expressed in presynaptic sensory neurons as well as in their postsynaptic spinal targets. We ablated *Bcl11a* selectively in pre- and postsynaptic neurons to determine the relative contribution of pre- versus postsynaptic expression of *Bcl11a* to sensory circuit formation. Genetic data presented in this study demonstrate that expression of *Bcl11a* in postsynaptic dorsal spinal neurons is required for the ingrowth of sensory afferents and for providing synaptic input to their targets. By contrast, *Bcl11a* expression in primary sensory neurons is dispensable for this process. This does not, however, exclude additional, as yet undetermined functions of *Bcl11a* in primary sensory neurons.

Somatosensory afferents are not equally affected by the mutation of *Bcl11a* in spinal neurons. Although sensory afferents expressing *TrkA*, aquaporin 1 or CGRP are strongly reduced in

the superficial dorsal horn, we do not detect major defects in proprioceptive fibers traveling to the ventral spinal cord. One explanation for this could be that only a few of their target neurons within the ventral spinal cord normally express *Bcl11a*. Thus, somatosensory neurons might differ in their dependence on *Bcl11a*. In addition, we detected all three major isoforms of *Bcl11a*, i.e. *Evi9a*, *b* and *c*, as being differentially expressed in the spinal cord. Whereas *Evi9b* is expressed throughout the spinal cord, *Evi9a* and *c* are predominantly expressed in the dorsal horn. Previous studies demonstrated that *Evi9* isoforms differ in their subcellular localization and biological activity (Nakamura et al., 2000; Kuo et al., 2009), raising the possibility that ingrowth of sensory afferents to the dorsal horn might depend on *Evi9a* and/or *c* selectively.

In addition to the innervation deficit, neurons of the dorsal spinal cord of *Bcl11a* mutants displayed disrupted morphogenesis and terminal differentiation. This raised the question of whether dorsal horn neurons require sensory innervation for correct maturation. However, *Sox10* mutants lack sensory neurons by E12.5 but do not display major deficits in the differentiation and morphogenesis of

**Fig. 7. Analysis of target gene expression in *Bcl11a* mutant dorsal spinal cord.**

(A,B) In situ hybridization analysis of *Frzb* mRNA expression in the dorsal horn of controls (A) and *Brn4-Cre* recombined *Bcl11a* mutants (B) at E14.5. Scale bar: 50 μ m.

(C) Determination of *Frzb* mRNA expression levels of control and mutant dorsal spinal cords by qRT-PCR at E14.5. Mean \pm s.e.m. *, *P*<0.05. (D) The *Frzb* promoter region indicating candidate regulatory regions (gray) as predicted by Ensembl Genome Browser and showing amplified fragments *Frzb1-3* used in ChIP analysis. The 5'UTR and ATG are indicated. Black arrowheads mark the boundaries of a *Frzb* promoter fragment used previously to drive transgenic *Frzb* expression in mice (Tylzanowski et al., 2004).

(E) ChIP assays on wild-type dorsal spinal cord tissue at E14.5 employing specific antibodies against *Bcl11a* or RNA polymerase II, and IgG as control. Binding of *Bcl11a* or RNA polymerase II to DNA was determined by qPCR using specific primer pairs for the *Frzb* promoter regions as indicated in D (region 1, +849 to +623; region 2, +138 to -27; region 3, -786 to -1008, relative to the transcription start site) as well as specific primer pairs amplifying the *Gapdh* and *Drg11* promoters. Pairwise comparison of ChIP data employing specific antibodies (RNA Pol AB, *Bcl11a* AB) versus IgG negative control was used for statistical analysis. Significantly more *Frzb* promoter DNA of regions 1 and 2 was recovered with the *Bcl11a* antibody than in controls Mean \pm s.e.m.; *n*=3. *, *P*<0.05 (Student's *t*-test); ns, not significant.

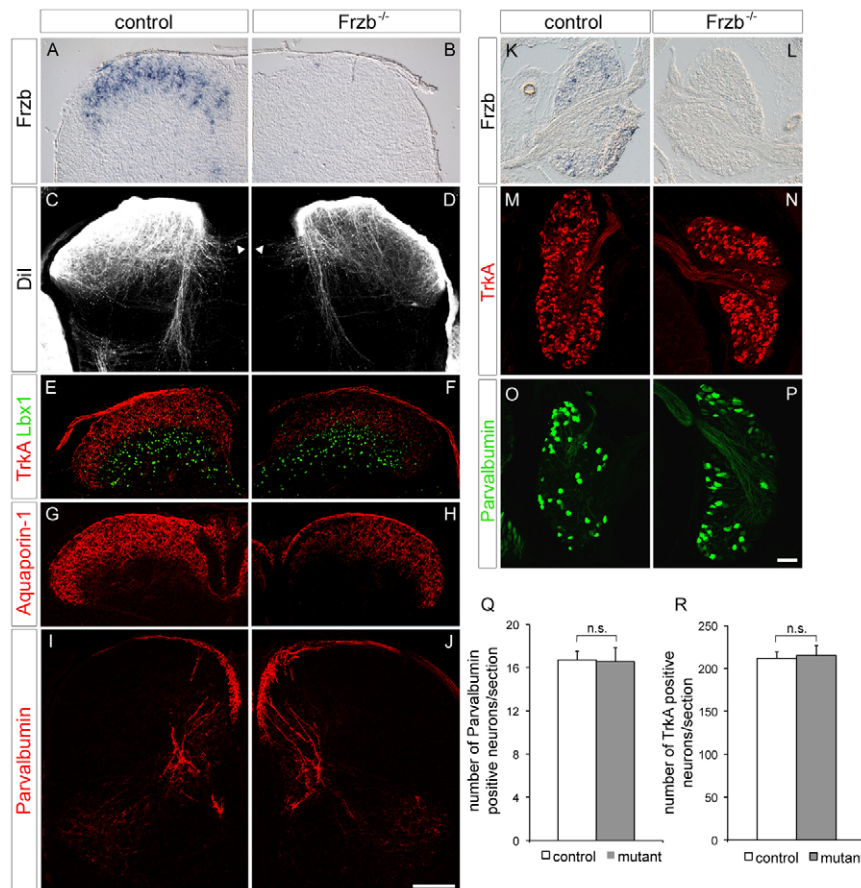


Fig. 8. Sensory axon projections in the *Frzb* mutant dorsal spinal horn. (A–J) Transverse sections of the dorsal horn of control (A, C, E, G, I) and *Frzb* mutant (B, D, F, H, J) mice at E16.5 (A–D) and E18.5 (E–J) hybridized with probes specific for *Frzb* (A, B) or stained with antibodies against TrkA (E, F), aquaporin 1 (G, H) or parvalbumin (I, J). Sensory axons entering the dorsal horn were traced with Dil (C, D). Axons crossing the midline are marked by arrowheads (C, D). (K–P) transverse sections of DRG of controls (K, M, O) and *Frzb* mutants (L, N, P) hybridized with *Frzb*-specific probes (K, L) or stained with antibodies against TrkA (M, N) and parvalbumin (O, P). (Q, R) Quantitative analysis of sensory neurons in DRG. Mean \pm s.e.m. n.s., not significant. Scale bars: 100 μ m in J; 50 μ m in P.

dorsal spinal neurons. Thus, the disrupted morphogenesis and differentiation of dorsal horn neurons in *Bcl11a* mutants is not caused by the deficit in sensory innervation.

Dendritic morphology and the presence of a particular transmitter receptor repertoire are important determinants of the number and type of presynaptic partners of a neuron (Hausser et al., 2000). Ingrowth of sensory afferents precedes terminal differentiation of spinal neurons (Ding et al., 2004). Thus, defective target differentiation, as observed in *Bcl11a* mutants, is unlikely to be the only cause for the deficit in dorsal horn innervation. We propose instead that Bcl11a regulates the expression of signals that guide somatosensory axons to their spinal targets. We identified such a guidance factor, Frzb, which was downregulated in the dorsal horn of *Bcl11a* mutants. The family of sFRPs function either as extracellular inhibitors of Wnt signaling or they can act independently of Wnt ligands. Wnt signals regulate multiple steps during the assembly of neural circuits (reviewed by Bovolenta et al., 2006; Salinas and Zou, 2008). In particular, sFRP1 acts as a guidance factor for retinal axons (Rodriguez et al., 2005). In addition, Wnts act as anterior-posterior guidance cues for commissural axons in the spinal cord, a function that is regulated by sFRPs (Lyuksyutova et al., 2003; Domanitskaya et al., 2010). Furthermore, neurite outgrowth of somatosensory neurons is controlled by the Wnt receptor Ryk (Lu et al., 2004).

We show that the disrupted Frzb expression is in part responsible for the deficit in sensory innervation of the dorsal horn of *Bcl11a* mutants. In particular, we observe reduced and disorganized cutaneous sensory innervation in the dorsal horn of *Frzb* mutants. Changes in the somatosensory system had not been noted previously in *Frzb* mutants (Lories et al., 2007). However, sensory

innervation deficits in *Frzb* mutants are milder than those in *Bcl11a* mutants, and the differentiation and morphogenesis of dorsal horn neurons appeared unaffected. This indicates that, in addition to *Frzb*, other genes exist that control neuronal development and are expressed in a Bcl11a-dependent manner.

Several lines of evidence suggest that *Frzb* is a direct target of Bcl11a: (1) Frzb was downregulated at early and late time points (E14.5 and E16.5) during development of the dorsal spinal cord of *Bcl11a* mutants, and Frzb expression did not depend on sensory innervation and was unchanged in *Sox10* mutants; (2) two distinct promoter fragments of *Frzb* are precipitated by ChIP with a Bcl11a-specific antibody; and (3) consensus binding sites for Bcl11a are present in the Frzb1 fragment. These experiments thus support a direct role of Bcl11a in the control of *Frzb*. Bcl11a was originally described as a COUP-TF-interacting protein (CTIP1). Mice with a targeted deletion of *COUP-TF1* (*Nr2f1* – Mouse Genome Informatics) display aberrant projections of cranial nerve axons (Qiu et al., 1997). COUP-TF1 is expressed in the developing spinal cord, and it is thus possible that Bcl11a cooperates with COUP-TF1 to regulate the differentiation of spinal neurons and sensory circuit formation.

A role for Bcl11a in neuronal morphogenesis

An important aspect of Bcl11a function in the dorsal horn is its role in neuronal morphogenesis. In the absence of Bcl11a, dorsal spinal neurons initiate neuritogenesis but form hypoplastic neurites with severely reduced branching complexity in vivo. A similar phenotype is observed when dorsal spinal neurons of *Bcl11a* mutants are cultured. It was previously reported that knockdown of Bcl11a-L (which corresponds to Evi9a in mice) in cultured rat

hippocampal neurons results in enhanced axonal branching and dendrite outgrowth, an effect that was proposed to be mediated by transcriptional control of *Dcc* and *Map1b* (Kuo et al., 2009). We did not detect changes in *Dcc* and *Map1b* (*Mtap1b* – Mouse Genome Informatics) expression in the spinal cord of *Bcl11a* mutant mice (data not shown). In our mutants, all three isoforms of *Bcl11a* were ablated from the genome. *Evi9a* and *Evi9b* are the major isoforms expressed in the murine hippocampus during development (Sebastian Karl and S.B., unpublished). Thus, the increase in neurite branching after knockdown of *Evi9a* might reflect residual *Evi9b* functions in rat hippocampal neurons in vitro, suggesting that the biological activities of *Bcl11a* are isoform specific (Nakamura et al., 2000; Kuo et al., 2009); they might also be neuron type specific.

In summary, we provide here a genetic characterization of the functions of the transcription factor *Bcl11a* in neuronal differentiation and the formation of sensory circuits. By the identification of *Frzb*, we link the transcriptional function of *Bcl11a* to its role in the guidance of sensory neurons.

Acknowledgements

We thank Jacqueline Andratschke and Verena Sasse (MDC, Berlin) for excellent technical assistance; Fritz Rathjen and Alistair Garratt (MDC, Berlin) for helpful discussions; Sebastian Karl and Michael Strehle (MDC, Berlin) for help with isoform-specific *Bcl11a* expression and microarray analysis, respectively; and Sylvie Dufour (Institut Curie, Paris), Tom Jessell (Columbia University, New York), Thomas Müller (MDC, Berlin) and Louis Reichardt (UCSF, San Francisco) for gifts of transgenic mice, antibodies and plasmids.

Funding

This work is supported by grants from the Deutsche Forschungsgemeinschaft [SFB497/A9 to S.B., DFG RA/5-1 to R.J.].

Competing interests statement

The authors declare no competing financial interests.

Supplementary material

Supplementary material available online at <http://dev.biologists.org/lookup/suppl/doi:10.1242/dev.072850/-DC1>

References

- Arlotta, P., Molyneaux, B. J., Chen, J., Inoue, J., Kominami, R. and Macklis, J. D. (2005). Neuronal subtype-specific genes that control corticospinal motor neuron development in vivo. *Neuron* **45**, 207-221.
- Arlotta, P., Molyneaux, B. J., Jabaudon, D., Yoshida, Y. and Macklis, J. D. (2008). *Ctip2* controls the differentiation of medium spiny neurons and the establishment of the cellular architecture of the striatum. *J. Neurosci.* **28**, 622-632.
- Avram, D., Fields, A., Pretty On Top, K., Nevriy, D. J., Ishmael, J. E. and Leid, M. (2000). Isolation of a novel family of C(2)H(2) zinc finger proteins implicated in transcriptional repression mediated by chicken ovalbumin upstream promoter transcription factor (COUP-TF) orphan nuclear receptors. *J. Biol. Chem.* **275**, 10315-10322.
- Avram, D., Fields, A., Senawong, T., Topark-Ngarm, A. and Leid, M. (2002). COUP-TF (chicken ovalbumin upstream promoter transcription factor)-interacting protein 1 (CTIP1) is a sequence-specific DNA binding protein. *Biochem. J.* **368**, 555-563.
- Baccei, M. L. and Fitzgerald, M. (2004). Development of GABAergic and glycinergic transmission in the neonatal rat dorsal horn. *J. Neurosci.* **24**, 4749-4757.
- Banker, G. and Goslin, K. (1998). *Culturing Nerve Cells*. Cambridge, MA: MIT Press.
- Bovolenta, P., Rodriguez, J. and Esteve, P. (2006). Frizzled/Ryk mediated signalling in axon guidance. *Development* **133**, 4399-4408.
- Brazma, A., Hingamp, P., Quackenbush, J., Sherlock, G., Spellman, P., Stoeckert, C., Aach, J., Ansorge, W., Ball, C. A., Causton, H. C. et al. (2001). Minimum information about a microarray experiment (MIAME)-toward standards for microarray data. *Nat. Genet.* **29**, 365-371.
- Britsch, S., Goerich, D. E., Riethmacher, D., Peirano, R. I., Rossner, M., Nave, K. A., Birchmeier, C. and Wegner, M. (2001). The transcription factor *Sox10* is a key regulator of peripheral glial development. *Genes Dev.* **15**, 66-78.
- Brown, A. G. (1981). *Organization of the Spinal Cord. The Anatomy and Physiology of Identified Neurons*. Heidelberg: Springer Verlag.
- Chen, Z., Luo, H. Y., Steinberg, M. H. and Chui, D. H. (2009). BCL11A represses HBG transcription in K562 cells. *Blood Cells Mol. Dis.* **42**, 144-149.
- Chen, Z. F., Rebelo, S., White, F., Malmberg, A. B., Baba, H., Lima, D., Woolf, C. J., Basbaum, A. I. and Anderson, D. J. (2001). The paired homeodomain protein DRG11 is required for the projection of cutaneous sensory afferent fibers to the dorsal spinal cord. *Neuron* **31**, 59-73.
- Cheng, L., Arata, A., Mizuguchi, R., Qian, Y., Karunaratne, A., Gray, P. A., Arata, S., Shirasawa, S., Bouchard, M., Luo, P. et al. (2004). *Tlx3* and *Tlx1* are post-mitotic selector genes determining glutamatergic over GABAergic cell fates. *Nat. Neurosci.* **7**, 510-517.
- Dasen, J. S. (2009). Transcriptional networks in the early development of sensory-motor circuits. *Curr. Top. Dev. Biol.* **87**, 119-148.
- Ding, Y. Q., Yin, J., Kania, A., Zhao, Z. Q., Johnson, R. L. and Chen, Z. F. (2004). *Lmx1b* controls the differentiation and migration of the superficial dorsal horn neurons of the spinal cord. *Development* **131**, 3693-3703.
- Domanitskaya, E., Wacker, A., Mauti, O., Baeriswyl, T., Esteve, P., Bovolenta, P. and Stoeckli, E. T. (2010). Sonic hedgehog guides post-crossing commissural axons both directly and indirectly by regulating Wnt activity. *J. Neurosci.* **30**, 11167-11176.
- Goulding, M., Lanuza, G., Sapir, T. and Narayan, S. (2002). The formation of sensorimotor circuits. *Curr. Opin. Neurobiol.* **12**, 508-515.
- Gross, M. K., Dottori, M. and Goulding, M. (2002). *Lbx1* specifies somatosensory association interneurons in the dorsal spinal cord. *Neuron* **34**, 535-549.
- Hausser, M., Spruston, N. and Stuart, G. J. (2000). Diversity and dynamics of dendritic signaling. *Science* **290**, 739-744.
- Heimrich, B. and Frotscher, M. (1991). Differentiation of dentate granule cells in slice cultures of rat hippocampus: a Golgi/electron microscopic study. *Brain Res.* **538**, 263-268.
- Helms, A. W. and Johnson, J. E. (2003). Specification of dorsal spinal cord interneurons. *Curr. Opin. Neurobiol.* **13**, 42-49.
- Iankova, I., Petersen, R. K., Annicotte, J. S., Chavey, C., Hansen, J. B., Kratchmarova, I., Sarruf, D., Benkirane, M., Kristiansen, K. and Fajas, L. (2006). Peroxisome proliferator-activated receptor gamma recruits the positive transcription elongation factor b complex to activate transcription and promote adipogenesis. *Mol. Endocrinol.* **20**, 1494-1505.
- Jawaid, K., Wahlberg, K., Thein, S. L. and Best, S. (2010). Binding patterns of BCL11A in the globin and GATA1 loci and characterization of the BCL11A fetal hemoglobin locus. *Blood Cells Mol. Dis.* **45**, 140-146.
- Kuo, T. Y., Hong, C. J. and Hsueh, Y. P. (2009). *Bcl11A/CTIP1* regulates expression of *DCC* and *MAP1b* in control of axon branching and dendrite outgrowth. *Mol. Cell. Neurosci.* **42**, 195-207.
- Liebel, J. T., Swandulla, D. and Zeilhofer, H. U. (1997). Modulation of excitatory synaptic transmission by nociceptin in superficial dorsal horn neurones of the neonatal rat spinal cord. *Br. J. Pharmacol.* **121**, 425-432.
- Liu, P., Jenkins, N. A. and Copeland, N. G. (2003a). A highly efficient recombineering-based method for generating conditional knockout mutations. *Genome Res.* **13**, 476-484.
- Liu, P., Keller, J. R., Ortiz, M., Tessarollo, L., Rachel, R. A., Nakamura, T., Jenkins, N. A. and Copeland, N. G. (2003b). *Bcl11a* is essential for normal lymphoid development. *Nat. Immunol.* **4**, 525-532.
- Livak, K. J. and Schmittgen, T. D. (2001). Analysis of relative gene expression data using real-time quantitative PCR and the 2(-Delta Delta C(T)) method. *Methods* **25**, 402-408.
- Lories, R. J., Peeters, J., Bakker, A., Tylzanowski, P., Derese, I., Schrooten, J., Thomas, J. T. and Luyten, F. P. (2007). Articular cartilage and biomechanical properties of the long bones in *Frzb*-knockout mice. *Arthritis Rheum.* **56**, 4095-4103.
- Lu, W., Yamamoto, V., Ortega, B. and Baltimore, D. (2004). Mammalian Ryk is a Wnt coreceptor required for stimulation of neurite outgrowth. *Cell* **119**, 97-108.
- Lyuksyutova, A. I., Lu, C. C., Milanesio, N., King, L. A., Guo, N., Wang, Y., Nathans, J., Tessier-Lavigne, M. and Zou, Y. (2003). Anterior-posterior guidance of commissural axons by Wnt-frizzled signaling. *Science* **302**, 1984-1988.
- Marmigere, F. and Ernfors, P. (2007). Specification and connectivity of neuronal subtypes in the sensory lineage. *Nat. Rev. Neurosci.* **8**, 114-127.
- Marmigere, F., Montelius, A., Wegner, M., Groner, Y., Reichardt, L. F. and Ernfors, P. (2006). The *Runx1/AML1* transcription factor selectively regulates development and survival of *TrkA* nociceptive sensory neurons. *Nat. Neurosci.* **9**, 180-187.
- Muller, T., Brohmann, H., Pierani, A., Heppenstall, P. A., Lewin, G. R., Jessell, T. M. and Birchmeier, C. (2002). The homeodomain factor *lhx1* distinguishes two major programs of neuronal differentiation in the dorsal spinal cord. *Neuron* **34**, 551-562.
- Nakamura, T., Yamazaki, Y., Saiki, Y., Moriyama, M., Largaespada, D. A., Jenkins, N. A. and Copeland, N. G. (2000). *Evi9* encodes a novel zinc finger protein that physically interacts with BCL6, a known human B-cell proto-oncogene product. *Mol. Cell. Biol.* **20**, 3178-3186.

- Oshio, K., Watanabe, H., Yan, D., Verkman, A. S. and Manley, G. T. (2006). Impaired pain sensation in mice lacking Aquaporin-1 water channels. *Biochem. Biophys. Res. Commun.* **341**, 1022-1028.
- Pecho-Vrieseling, E., Sigrist, M., Yoshida, Y., Jessell, T. M. and Arber, S. (2009). Specificity of sensory-motor connections encoded by Sema3e-Pixnd1 recognition. *Nature* **459**, 842-846.
- Pietri, T., Eder, O., Blanche, M., Thiery, J. P. and Dufour, S. (2003). The human tissue plasminogen activator-Cre mouse: a new tool for targeting specifically neural crest cells and their derivatives in vivo. *Dev. Biol.* **259**, 176-187.
- Qian, Y., Shirasawa, S., Chen, C. L., Cheng, L. and Ma, Q. (2002). Proper development of relay somatic sensory neurons and D2/D4 interneurons requires homeobox genes Rnx/Tlx-3 and Tlx-1. *Genes Dev.* **16**, 1220-1233.
- Qiu, Y., Pereira, F. A., DeMayo, F. J., Lydon, J. P., Tsai, S. Y. and Tsai, M. J. (1997). Null mutation of mCOUP-TF1 results in defects in morphogenesis of the glossopharyngeal ganglion, axonal projection, and arborization. *Genes Dev.* **11**, 1925-1937.
- Rodriguez, J., Esteve, P., Weinl, C., Ruiz, J. M., Fermin, Y., Trousse, F., Dwivedy, A., Holt, C. and Bovolenta, P. (2005). SFRP1 regulates the growth of retinal ganglion cell axons through the Fz2 receptor. *Nat. Neurosci.* **8**, 1301-1309.
- Salinas, P. C. and Zou, Y. (2008). Wnt signaling in neural circuit assembly. *Annu. Rev. Neurosci.* **31**, 339-358.
- Sankaran, V. G., Menne, T. F., Xu, J., Akie, T. E., Lettre, G., Van Handel, B., Mikkola, H. K., Hirschhorn, J. N., Cantor, A. B. and Orkin, S. H. (2008). Human fetal hemoglobin expression is regulated by the developmental stage-specific repressor BCL11A. *Science* **322**, 1839-1842.
- Sankaran, V. G., Xu, J., Ragoczy, T., Ippolito, G. C., Walkley, C. R., Maika, S. D., Fujiwara, Y., Ito, M., Groudine, M., Bender, M. A. et al. (2009). Developmental and species-divergent globin switching are driven by BCL11A. *Nature* **460**, 1093-1097.
- Schmidt, H., Stonkute, A., Juttner, R., Schaffer, S., Buttgereit, J., Feil, R., Hofmann, F. and Rathjen, F. G. (2007). The receptor guanylyl cyclase Npr2 is essential for sensory axon bifurcation within the spinal cord. *J. Cell Biol.* **179**, 331-340.
- Schwenk, F., Baron, U. and Rajewsky, K. (1995). A cre-transgenic mouse strain for the ubiquitous deletion of loxP-flanked gene segments including deletion in germ cells. *Nucleic Acids Res.* **23**, 5080-5081.
- Sholl, D. A. (1953). Dendritic organization in the neurons of the visual and motor cortices of the cat. *J. Anat.* **87**, 387-406.
- Sun, Y. G. and Chen, Z. F. (2007). A gastrin-releasing peptide receptor mediates the itch sensation in the spinal cord. *Nature* **448**, 700-703.
- Tylzanowski, P., Bossuyt, W., Thomas, J. T. and Luyten, F. P. (2004). Characterization of Frzb-Cre transgenic mouse. *Genesis* **40**, 200-204.
- Vrieseling, E. and Arber, S. (2006). Target-induced transcriptional control of dendritic patterning and connectivity in motor neurons by the ETS gene Pea3. *Cell* **127**, 1439-1452.
- Wine-Lee, L., Ahn, K. J., Richardson, R. D., Mishina, Y., Lyons, K. M. and Crenshaw, E. B., 3rd (2004). Signaling through BMP type 1 receptors is required for development of interneuron cell types in the dorsal spinal cord. *Development* **131**, 5393-5403.
- Xu, Y., Lopes, C., Qian, Y., Liu, Y., Cheng, L., Goulding, M., Turner, E. E., Lima, D. and Ma, Q. (2008). Tlx1 and Tlx3 coordinate specification of dorsal horn pain-modulatory peptidergic neurons. *J. Neurosci.* **28**, 4037-4046.
- Yoshida, Y., Han, B., Mendelsohn, M. and Jessell, T. M. (2006). PlexinA1 signaling directs the segregation of proprioceptive sensory axons in the developing spinal cord. *Neuron* **52**, 775-788.

Differential gene expression in *Bcl11a* mutant dorsal spinal cord

| Affymetrix ID | Gene symbol | Genbank ID | Change <i>P</i> -value | Fold-change |
|----------------------------|----------------------|------------|------------------------|--------------|
| Downregulated genes | | | | |
| 1447334_at | <i>Bcl11a</i> | BB526119 | 4.81E-08 | -13.45414464 |
| 1419406_a_at | <i>Bcl11a</i> | NM_016707 | 4.73E-08 | -8.116123948 |
| 1450260_at | <i>Grpr</i> | M57922 | 3.67E-05 | -6.204484917 |
| 1457072_at | <i>Bcl11a</i> | BF731393 | 7.75E-08 | -5.453025359 |
| 1456632_at | <i>Bcl11a</i> | BB424718 | 1.41E-08 | -5.36405061 |
| 1446293_at | <i>Bcl11a</i> | BB471990 | 4.43E-05 | -4.796960888 |
| 1428642_at | <i>Slc35d3</i> | AK018094 | 6.14E-05 | -3.589984253 |
| 1422825_at | <i>Cart</i> | NM_013732 | 4.59E-05 | -2.882588616 |
| 1457797_at | <i>Slc8a1</i> | AV340788 | 1.51E-05 | -2.674092389 |
| 1446622_at | <i>A330068G13Rik</i> | BB191623 | 2.24E-05 | -2.24557795 |
| 1416658_at | <i>Frzb</i> | U91905 | 9.01E-07 | -2.239973937 |
| 1432825_at | <i>2900018N21Rik</i> | AK013552 | 2.44E-05 | -2.239020383 |
| 1438239_at | <i>Mid1</i> | BG073178 | 6.4E-05 | -2.153784217 |
| 1433701_at | <i>Mpped1</i> | BB371430 | 2.11E-05 | -2.051349964 |
| 1452656_at | <i>Zdhhc2</i> | BB224658 | 7.02E-05 | -1.96649857 |
| 1436035_at | <i>3830431G21Rik</i> | AV225683 | 1.06E-05 | -1.962778283 |
| 1426047_a_at | <i>Ptprr</i> | AF129509 | 6.32E-05 | -1.941226429 |
| 1460668_at | <i>Gal</i> | NM_010253 | 2.87E-05 | -1.937069656 |
| 1455869_at | <i>Camk2b</i> | BG862223 | 5.72E-05 | -1.913351264 |
| 1418161_at | <i>Jph3</i> | NM_020605 | 1.30E-05 | -1.905919862 |
| 1445589_at | <i>Slc23a2</i> | BM940232 | 5.47E-05 | -1.902432029 |
| 1434776_at | <i>Sema5a</i> | BQ176610 | 6.04E-05 | -1.86572666 |
| 1437319_at | <i>D9Ertd414e</i> | BG069400 | 1.54E-05 | -1.865635356 |
| 1453098_at | <i>Gria2</i> | AK014389 | 1.82E-05 | -1.863601115 |
| 1437422_at | <i>Sema5a</i> | AV375653 | 7.67E-05 | -1.855922895 |

| Affymetrix ID | Gene symbol | Genbank ID | Change <i>P</i> -value | Fold-change |
|--------------------------|-----------------|------------|------------------------|-------------|
| Upregulated genes | | | | |
| 1450736_a_at | <i>Hbb-bh1</i> | NM_008219 | 2.20E-09 | 35.61121791 |
| 1437990_x_at | <i>Hbb-bh1</i> | AV147727 | 9.03E-09 | 35.26825279 |
| 1437810_a_at | <i>Hbb-bh1</i> | AV311770 | 2.67E-07 | 34.62677676 |
| 1429517_at | <i>Zfyve20</i> | BC017622 | 3.19E-05 | 7.109685906 |
| 1432589_at | <i>Plcg1</i> | BF166706 | 2.81E-07 | 7.013992117 |
| 1430391_a_at | <i>St8sia4</i> | AK003690 | 2.91E-06 | 6.301004155 |
| 1420230_at | <i>AA414993</i> | AA414993 | 2.61E-06 | 6.009843385 |
| 1431196_at | <i>Atp2c1</i> | BG296252 | 2.40E-06 | 4.728163341 |
| 1449885_at | <i>Tmem47</i> | NM_138751 | 1.43E-07 | 4.722526295 |
| 1429385_at | <i>Wdr68</i> | BI082535 | 2.49E-06 | 4.272174849 |
| 1448716_at | <i>Hba-x</i> | M26898 | 6.16E-07 | 4.213009015 |
| 1452638_s_at | <i>Dnm1l</i> | BC027538 | 1.35E-05 | 4.004418365 |
| 1456255_at | <i>AI314180</i> | BB553400 | 1.01E-06 | 3.965965013 |
| 1437257_at | <i>Wdr47</i> | BB344753 | 1.50E-08 | 3.95664415 |
| 1451610_at | <i>ECM29l</i> | BC024561 | 6.51E-06 | 3.952606098 |
| 1427430_at | <i>AI848100</i> | BB148987 | 5.43E-05 | 3.894914242 |
| 1431064_at | <i>Dpp8</i> | BF119821 | 1.64E-05 | 3.802372114 |
| 1420652_at | <i>Ate1</i> | BE309332 | 3.60E-05 | 3.642381587 |
| 1448458_at | <i>Top2b</i> | BB166592 | 5.88E-07 | 3.634330961 |

| | | | | |
|--------------|-----------------|-----------|----------|-------------|
| 1426505_at | <i>Evi2b</i> | AI122415 | 8.92E-06 | 3.632934073 |
| 1424570_at | <i>Ddx46</i> | BF023426 | 2.40E-05 | 3.55541412 |
| 1416660_at | <i>Eif3s10</i> | AW701127 | 5.64E-05 | 3.506743664 |
| 1423325_at | <i>Pnn</i> | AV135835 | 1.05E-05 | 3.497019017 |
| 1444199_at | <i>Elk4</i> | AW046689 | 3.97E-05 | 3.477198429 |
| 1419519_at | <i>Igf1</i> | NM_010512 | 2.75E-05 | 3.421510667 |
| 1421248_at | <i>Syn3</i> | NM_013722 | 2.97E-07 | 3.301289723 |
| 1456343_at | <i>Slc35f1</i> | BB540579 | 2.48E-05 | 3.282755202 |
| 1450087_a_at | <i>Nolc1</i> | NM_053086 | 7.53E-06 | 3.226996335 |
| 1427830_at | <i>Zfp260</i> | L36316 | 7.67E-05 | 3.226275533 |
| 1435872_at | <i>Pim1</i> | BE631223 | 3.29E-05 | 3.216496521 |
| 1442766_at | <i>Ppp4r1</i> | AI846596 | 1.01E-05 | 3.206447054 |
| 1434419_s_at | <i>Tardbp</i> | AW538183 | 3.15E-05 | 3.189801662 |
| 1444904_at | <i>Cbfa2t1h</i> | BG068236 | 5.63E-05 | 3.177284101 |
| 1428017_at | <i>Pknox2</i> | AF487460 | 1.35E-06 | 3.162853048 |
| 1447871_at | <i>Mtx2</i> | BI714072 | 5.88E-07 | 3.061908909 |
| 1450321_at | <i>Zfp354c</i> | NM_013922 | 1.26E-05 | 3.057033256 |
| 1416019_at | <i>Dr1</i> | NM_026106 | 1.79E-06 | 3.046954246 |
| 1433804_at | <i>Jak1</i> | BQ032637 | 4.48E-05 | 2.907430036 |
| 1416748_a_at | <i>Mre11a</i> | NM_018736 | 2.58E-06 | 2.888036044 |
| 1460304_a_at | <i>Ubtf</i> | BB832806 | 2.10E-05 | 2.879600247 |
| 1444536_at | <i>AI462171</i> | AI462171 | 1.89E-05 | 2.878207922 |
| 1440984_at | <i>Baz2b</i> | BE943712 | 5.30E-05 | 2.869833884 |
| 1455658_at | <i>Cggbp1</i> | BI080272 | 1.05E-06 | 2.864477895 |
| 1431338_at | <i>Caskin1</i> | AK014376 | 2.90E-05 | 2.863331895 |
| 1419425_at | <i>Cnr1</i> | NM_007726 | 6.34E-08 | 2.851835278 |
| 1443522_s_at | <i>Phip</i> | BM221262 | 1.14E-05 | 2.850630874 |
| 1418889_a_at | <i>Csnk1d</i> | NM_139059 | 6.42E-05 | 2.82555789 |
| 1453590_at | <i>Arl5b</i> | BQ032239 | 4.07E-05 | 2.810921874 |
| 1445238_at | <i>Ccl21b</i> | BB239244 | 1.25E-06 | 2.772489491 |
| 1449504_at | <i>Kpna1</i> | U20619 | 3.21E-05 | 2.768349436 |
| 1419344_at | <i>Tcte1</i> | NM_013688 | 3.98E-05 | 2.761346663 |
| 1424325_at | <i>Esco1</i> | BB308198 | 9.93E-05 | 2.746473362 |
| 1425515_at | <i>Pik3r1</i> | M60651 | 3.54E-05 | 2.69283597 |
| 1450243_a_at | <i>Dscr111</i> | NM_030598 | 2.66E-07 | 2.684780535 |
| 1420899_at | <i>Rab18</i> | AW542340 | 6.42E-05 | 2.67333255 |
| 1449548_at | <i>Efnb2</i> | U30244 | 1.81E-05 | 2.669096203 |
| 1420816_at | <i>Ywhag</i> | NM_018871 | 3.83E-05 | 2.649034404 |
| 1444996_at | <i>Depdc5</i> | BG067666 | 1.30E-06 | 2.629950635 |
| 1446926_at | <i>Pycard</i> | AU040917 | 1.05E-06 | 2.617144887 |
| 1431274_a_at | <i>Hspa9a</i> | AA543265 | 2.13E-06 | 2.583065882 |
| 1446682_at | <i>Zswim6</i> | BB660139 | 6.46E-05 | 2.564815322 |
| 1449949_a_at | <i>Cxadr</i> | U90715 | 7.14E-05 | 2.542242336 |
| 1459648_at | <i>Rutbc3</i> | BE627992 | 1.14E-05 | 2.498150765 |
| 1432344_a_at | <i>Aplp2</i> | AK013376 | 2.28E-06 | 2.497216168 |
| 1446484_at | <i>Mef2c</i> | BB558401 | 8.13E-06 | 2.490409664 |
| 1415773_at | <i>Ncl</i> | BF118393 | 1.80E-06 | 2.484618366 |
| 1421477_at | <i>Cplx2</i> | NM_009946 | 6.42E-06 | 2.479666949 |
| 1435009_at | <i>Slc9a6</i> | BB611738 | 1.11E-05 | 2.455488305 |
| 1423214_at | <i>Plxnc1</i> | BB476707 | 1.93E-05 | 2.387979685 |
| 1424332_at | <i>Rab40c</i> | AF422144 | 8.06E-05 | 2.358015469 |
| 1456651_a_at | <i>Tpr</i> | BG067858 | 4.77E-06 | 2.356109997 |
| 1423329_at | <i>Gdap1</i> | AU017649 | 1.90E-05 | 2.350862988 |
| 1416043_at | <i>Nasp</i> | BB493242 | 3.65E-05 | 2.335816875 |

| | | | | |
|--------------|------------------|-----------|----------|-------------|
| 1455748_at | <i>Gpr178</i> | AI662241 | 2.74E-05 | 2.333911832 |
| 1417781_at | <i>Lass4</i> | BB006809 | 1.30E-05 | 2.333638981 |
| 1420982_at | <i>Rnpc2</i> | NM_133242 | 2.37E-05 | 2.310019202 |
| 1450522_a_at | <i>H1f0</i> | NM_008197 | 5.74E-05 | 2.306425231 |
| 1454304_at | <i>Epn2</i> | BB626346 | 2.64E-05 | 2.287035859 |
| 1460131_at | <i>Rnf170</i> | BG067721 | 1.48E-05 | 2.238187031 |
| 1450392_at | <i>Abca1</i> | BB144704 | 2.52E-05 | 2.212401088 |
| 1426714_at | <i>D11Ert18e</i> | AK003278 | 3.14E-06 | 2.190147066 |
| 1427408_a_at | <i>Thrap3</i> | BC012655 | 2.24E-06 | 2.177392372 |
| 1426715_s_at | <i>D11Ert18e</i> | AK003278 | 3.59E-05 | 2.150738751 |
| 1421789_s_at | <i>Arf3</i> | NM_007478 | 9.78E-07 | 2.147247301 |
| 1440228_at | <i>Ranbp6</i> | BB477637 | 4.80E-06 | 2.143338627 |
| 1427638_at | <i>Zbtb16</i> | Z47205 | 8.42E-06 | 2.141114995 |
| 1425597_a_at | <i>Qk</i> | AW060288 | 2.42E-05 | 2.126582508 |
| 1442872_at | <i>BC021438</i> | BB022993 | 5.72E-06 | 2.09856836 |
| 1451730_at | <i>Zfp62</i> | BC022935 | 4.90E-05 | 2.090004098 |
| 1425713_a_at | <i>Rnf146</i> | BC019182 | 3.43E-05 | 2.089779763 |
| 1425490_a_at | <i>Wdr13</i> | AK017549 | 1.85E-06 | 2.082986698 |
| 1438686_at | <i>Eif4g1</i> | BB531220 | 5.31E-05 | 2.074047996 |
| 1454107_a_at | <i>Kif2a</i> | AK016720 | 2.30E-05 | 2.070858853 |
| 1450762_s_at | <i>Zfp191</i> | BF780333 | 7.83E-05 | 2.051713553 |
| 1450407_a_at | <i>Anp32a</i> | AF022957 | 6.35E-06 | 2.040646039 |
| 1421339_at | <i>Extl3</i> | NM_018788 | 4.81E-05 | 2.006553153 |
| 1458676_at | <i>Nktr</i> | BB712791 | 3.42E-05 | 2.00603001 |
| 1431328_at | <i>Ppp1cb</i> | AK017392 | 2.73E-05 | 2.000893152 |
| 1425631_at | <i>Ppp1r3c</i> | U89924 | 2.86E-05 | 1.99903859 |
| 1448127_at | <i>Rrm1</i> | BB758819 | 9.49E-05 | 1.993870937 |
| 1443878_at | <i>Rapgef6</i> | BB306768 | 2.65E-05 | 1.99328962 |
| 1434282_at | <i>Ibtk</i> | BM250711 | 4.11E-05 | 1.988935323 |
| 1460426_at | <i>Pde4dip</i> | AI639670 | 3.06E-06 | 1.984632664 |
| 1416701_at | <i>Rnd3</i> | BC009002 | 1.64E-05 | 1.983916553 |
| 1449578_at | <i>Supt16h</i> | AW536705 | 2.11E-05 | 1.973119101 |
| 1431030_a_at | <i>Rnf14</i> | AK010162 | 2.65E-05 | 1.970928939 |
| 1425624_at | <i>Epm2aip1</i> | BC018474 | 9.24E-05 | 1.962687538 |
| 1460386_a_at | <i>Slc1a1</i> | AF087578 | 2.41E-05 | 1.955461765 |
| 1444333_at | <i>Strn3</i> | BB485260 | 1.93E-05 | 1.955034629 |
| 1458685_at | <i>Garnl1</i> | BB552367 | 1.65E-05 | 1.953421381 |
| 1442629_at | <i>Nt5c2</i> | AU017183 | 6.50E-05 | 1.951756982 |
| 1456104_at | <i>Psm11</i> | BE949498 | 6.46E-05 | 1.950168902 |
| 1426744_at | <i>Srebf2</i> | BM123132 | 2.79E-05 | 1.943511478 |
| 1442404_at | <i>Ncl</i> | BB624790 | 2.61E-05 | 1.943410453 |
| 1415795_at | <i>Spin</i> | BM228780 | 1.83E-05 | 1.942326357 |
| 1447924_at | <i>Nucks1</i> | AW048468 | 1.07E-06 | 1.942215708 |
| 1417755_at | <i>Topors</i> | NM_134097 | 7.31E-05 | 1.939400843 |
| 1439042_at | <i>Adcyap1r1</i> | BB427884 | 6.38E-05 | 1.937250691 |
| 1452430_s_at | <i>Sfrs1</i> | X66091 | 6.39E-05 | 1.917936232 |
| 1453853_a_at | <i>Arhgef12</i> | AI481688 | 2.04E-05 | 1.913243672 |
| 1425329_a_at | <i>Cyb5r3</i> | AF332060 | 4.23E-05 | 1.90763443 |
| 1451762_a_at | <i>Kif1b</i> | AB023656 | 5.13E-05 | 1.904250658 |
| 1416732_at | <i>Top2b</i> | BB166592 | 1.20E-05 | 1.900368892 |

Systematic analysis of gene expression in control and Brn4-Cre recombined *Bcl11a* mutant spinal cords using Affymetrix oligonucleotide microarrays (MOE 430 2.0 Gene Chip). Expression profiles were determined at E16.5. The average signal fold change and the change *P*-value from three replicates are shown. Genes were selected based on the following cut-offs: fold change ≥ 1.9 for upregulated genes and ≤ -1.9 for those downregulated in mutants; change *P*-value ≤ 0.0001 .